SCIENTIFIC REPORTS

OPEN

SUBJECT AREAS:
SMALL MOLECULES
DRUG DISCOVERY
BIOPHYSICAL CHEMISTRY

Received
7 October 2013

Accepted
6 January 2014

Published
27 January 2014

Correspondence and requests for materials should be addressed to A.K.T. (akthakur@iitk.ac.in)

Therapeutic implication of L-phenylalanine aggregation mechanism and its modulation by D-phenylalanine in phenylketonuria

Virender Singh[1], Ratan Kumar Rai[2], Ashish Arora[3], Neeraj Sinha[2] & Ashwani Kumar Thakur[1]

[1]Department of Biological Sciences and Bioengineering, Indian Institute of Technology Kanpur 208016, Uttar Pradesh, India, [2]Centre of Biomedical Research, SGPGIMS Campus, Raibarelly Road, Lucknow 226014, Uttar Pradesh, India, [3]CSIR-Central Drug Research Institute, 10/1, Sector 10, Jankipuram Extension, Sitapur Road, Lucknow 226031, Uttar Pradesh, India.

Self-assembly of phenylalanine is linked to amyloid formation toxicity in phenylketonuria disease. We are demonstrating that L-phenylalanine self-assembles to amyloid fibrils at varying experimental conditions and transforms to a gel state at saturated concentration. Biophysical methods including nuclear magnetic resonance, resistance by alpha-phenylglycine to fibril formation and preference of protected phenylalanine to self-assemble show that this behaviour of L-phenylalanine is governed mainly by hydrophobic interactions. Interestingly, D-phenylalanine arrests the fibre formation by L-phenylalanine and gives rise to flakes. These flakes do not propagate further and prevent fibre formation by L-phenylalanine. This suggests the use of D-phenylalanine as modulator of L-phenylalanine amyloid formation and may qualify as a therapeutic molecule in phenylketonuria.

Phenylketonuria (PKU) is an inborn metabolic disorder linked with inability of infants to utilize phenylalanine (Phe) due to lack of phenylalanine hydroxylase (PAH) enzyme activity caused by a genetic mutation[1]. This drastically increases blood Phe concentration from normal 50 $\mu M\,L^{-1}$ to toxic 1200 $\mu M\,L^{-1}$ level[2–4]. As a result there is a deficit of tyrosine, dopamine, epinephrine and norepinephrine molecules[1]. This hampers proper brain development and results in psychiatric disorder in patients[2,3]. Currently, restricted Phe diet along with large neutral amino acids (LNAA) and tetrahydrobiopterin therapy are used to reduce toxic effects in PKU patients[2].

Recently, Adler *et al.* for the first time linked Phe self-assembly with PKU[5]. High build-up of Phe in hippocampus and the parietal cortex area of the brain, results in self-assembly and fibril formation. Birefringence characteristic upon congo red dye binding, thioflavin T (ThT) binding and electron diffraction confirmed that these fibres are amyloidic in nature[5]. Phe fibres have shown the characteristic cross β-fibre diffraction pattern present in amyloid fibrils[6], associated with several neurodegenerative diseases like Alzheimer's disease, Huntington's disease and Atrial amyloidosis[7]. Presence of these amyloids and intermediate oligomers in different regions of brain are associated with toxicity, leading to neuronal death[6,8]. Phe fibres showed similar cell toxicity on PC12 and Chinese Hamster Ovary (CHO) cells[5]. Importantly, the antibody and histological staining of brain tissues from PKU patients have shown the presence of Phe fibrils, indicating amyloid fibril associated toxicity[5]. Similar, needle like fibrillar morphology was observed under optical microscope for Phe crystals while studying aspartame gel crystallization[9]. Phe also form dimers in presence of its cationic and zwitterionic state in aqueous solution[10].

It was estimated by using infrared spectroscopy that the interactions responsible for Phe assembly are mainly hydrogen bonding between symmetrical –C=O···HOOC– and electrostatic between $-NH_3^+\cdots{}^-OOC-$ groups[5,11]. However, it seems a reasonable assumption that Phe being an aromatic amino acid can also form hydrophobic interactions through π-π stacking. Involvement of these interactions are not established completely, but are predicted to favour self-assembly[10]. Also, self-assembly of diphenylalanine suggests the importance of stacking interactions in stabilizing nanostructures[12]. The π-π stacking interactions leading to association of aromatic side chain of Phe are involved in molecular recognition[13], peptide self-assembly to fibril formation[14–16] and neurotoxicity[17].

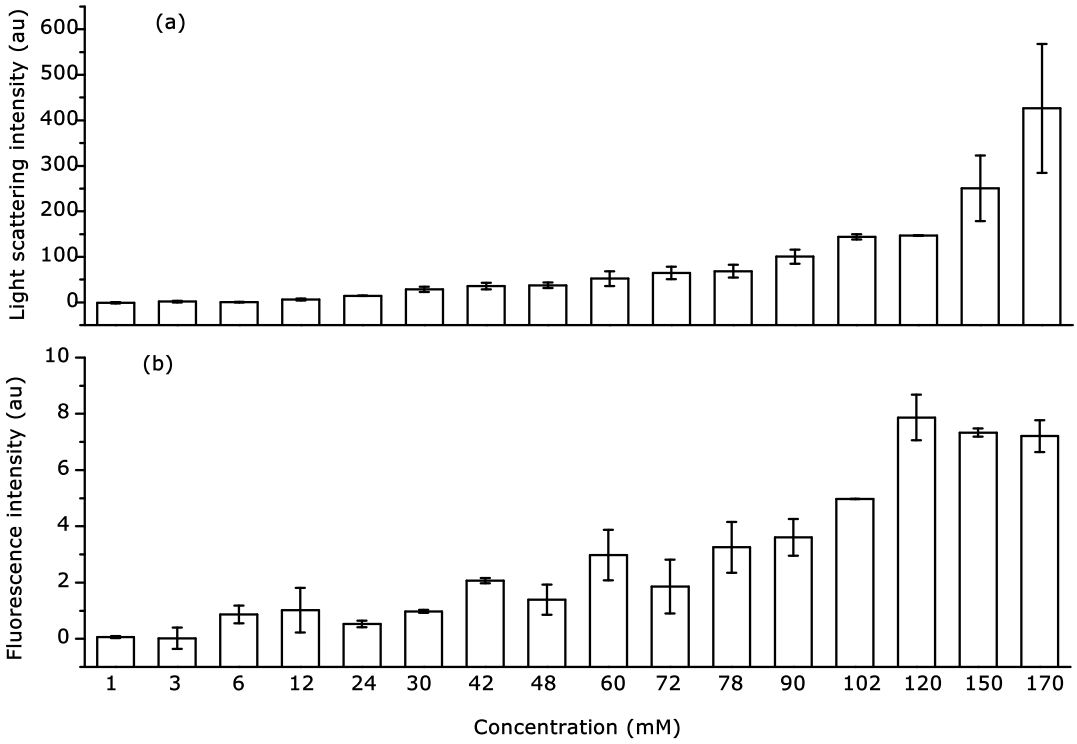

Figure 1 | (a) Light scattering and (b) Thioflavin T binding assay of L-Phe in water at different concentrations.

The studies mentioned above qualify that Phe forms fibrous material and its importance in disease association. However, the mechanism of their formation is not completely deciphered. In this paper, Phe self-assembly and mechanism leading to fibre formation are reported. Apart from earlier known interactions in Phe self-assembly, we present here the major role played by hydrophobic interactions involving Phe ring in this process. We have further demonstrated inhibition of L-Phe fibrillar assemblies by D-Phe enantiomer to non-propagating flakes. This study provides one useful strategy for arresting the amyloid fibre formation in phenylketonuria disease.

Results

Kinetics of phe self-assembly. L-Phe self-assembly was monitored by light scattering (LS) and thioflavin t (ThT) binding assays. Samples in water (pH 5.8 ± 0.3) at different concentrations were used. An increase in light scattering was observed beyond 60 mM and sudden increase after 120 mM concentration representing self-assembly process (Fig. 1a). These assemblies were tested for ThT binding and showed enhanced fluorescence above 3 mM concentration (Fig. 1b). The similar trend for ThT binding and light scattering was not observed in L-glutamine (L-Gln) (Supplementary Fig. S1). We have also observed increase in particle size of L-Phe with increasing concentration by dynamic light scattering measurement (DLS) (Supplementary Fig. S2).

In order to determine kinetics of self-assembly to fibre formation, saturated concentration (300 mM) of Phe was chosen. This solution of L-Phe was prepared in water and phosphate buffered saline (PBS) at 70 °C. The clear transition from the solution phase to gel was observed on cooling it to room temperature (Fig. 2a). Similar effect was observed during aspartame and Phe gel crystallization studies but without kinetic information[9]. Kinetics observed by light scattering

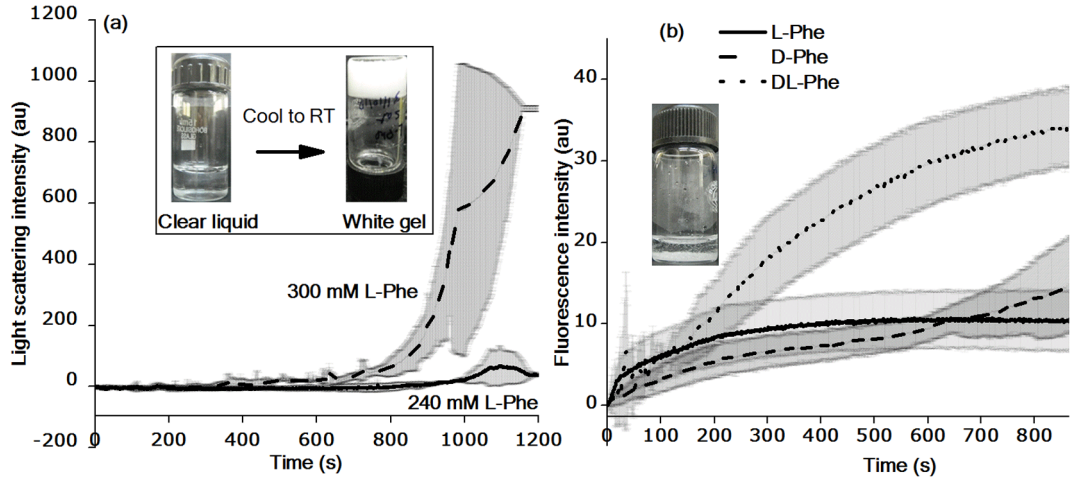

Figure 2 | (a) Gel formation kinetics of L-Phe. Self supporting gel of L-Phe on cooling saturated solution (300 mM) at room temperature (inset) (b) Self-assembly kinetics of L, D and DL-Phe monitored by thioflavin T (ThT) binding fluorescence assay. Sedimented particles of DL-Phe (inset).

analysis showed the appearance of a lag phase followed by an exponential phase (Fig. 2a). An initial lag might be due to nucleation events where molecules associate to form productive nucleus for further elongation into mature fibres or the associated molecules are insensitive to light scattering. In such case, seeding with preformed aggregates could abrogate this phase and the reaction will seed quickly for elongation[18].

When 10% (w/w) preformed L-Phe aggregates were incubated with saturated L-Phe solution, it abolished lag phase and gel formation was so quick that it was practically difficult to monitor it by light scattering and ThT binding due to signal saturation. This is an interesting finding in Phe assembly. Similar behaviour of lag and elongation phase was reported for amyloid forming peptides[19] such as polyglutamine in Huntington's disease[18]. Interestingly, ThT binding assay showed enhanced fluorescence even at earlier time points and lower concentrations suggesting early formation of ThT positive assemblies (Fig. 1b and Fig. 2b) which corroborates well with DLS data (Supplementary Fig. S2). L-Phe in PBS buffer showed similar kinetics and gel formation behaviour as in water (Supplementary Fig. S3). Hence, water was used for further molecular interaction studies as also used by Adler *et al.* for most experiments[5].

Aggregate structure and mechanism of phe aggregation. To understand the morphology of Phe assemblies, scanning electron microscopy (SEM) was performed. Long fibrous structures were observed at low (300 μM) and high concentrations (6 mM–300 mM) (Fig. 3a and 3b). These morphologies are quite similar to those observed in PKU mouse model and patient brain tissues[5]. Needle like fibrous morphology was observed at 1,000× magnification formed at saturated concentration (Fig. 3c). Interestingly, at higher magnification (10,000×), they look like tubular structures (Fig. 3c). Fibrils are characterized with 0.2–2 μm diameter and 100–300 μm length.

Self-assembly mechanism of peptides and proteins is governed by different non-covalent interactions[20]. In Phe, the possibility of intermolecular electrostatic interactions between $-NH_3^+\cdots{}^-OOC-$ and hydrogen bonding between –C=O···HOOC– groups were shown by infrared spectroscopy and π-π stacking interactions were predicted between phenyl rings[5,11]. To find the role of these interactions in self-assembly, we followed different strategies. Phe being in zwitterionic state at pH 5.5, it is possible that self-assembly can occur due to electrostatic interactions. At pH 2, it behaves majorly as cation and around pH 9 as anion[21]. At these extreme pH values, solubility of Phe should increase and diminish the gel formation tendency. Interestingly, gel formation was observed at both low and high pH values but with longer time (24 h) as compared to pH 5.5 (1–2 h). SEM images revealed similar fibrous morphologies at low pH (Fig. 3g), in PBS (neutral pH) (Fig. 3f) and at isoelectric pH (Fig. 3c) with the only variation in alkaline pH where long multinodal fibres were observed (Fig. 3h).

To probe into the role of hydrophobic regions in fibrous state, ANS (8-anilino-1-naphthalenesulfonic acid) binding assay was carried out[22,23]. ANS works as a surface hydrophobic probe with typical behaviour of change in fluorescence on changing its environment from hydrophilic to hydrophobic[24]. With increasing concentration of L-Phe from 6 mM to 300 mM, an increase in ANS fluorescence intensity was observed (Supplementary Fig. S4). Dose dependent increase in fluorescence indicates the presence of more hydrophobic regions[25]. In contrast, no increase in ANS fluorescence was observed for glutamine with increasing concentration (Supplementary Fig. S5a). Also the effect is specific to aggregation of Phe as in guanidine hydrochloride (GuHCl), increase in ANS fluorescence was not observed (Supplementary Fig. S5b). GuHCl as a denaturant, perturbed the hydrophobic interactions and hence self-assembly of Phe[26,27].

To further highlight the involvement of hydrophobic interactions, we carried out concentration dependent ^{1}H NMR of L-Phe. With increasing concentration from 6 mM to 150 mM, an upfield shift was observed for aryl protons (Fig. 4a). This upfield shift suggests screening of aryl protons due to stacking of aromatic rings upon self-association of Phe molecules[28]. This is further supported by similar chemical shift for phenyl carbon in ^{13}C NMR (Fig. 4b). Further to characterize self-assembly, diffusion-ordered spectroscopy (DOSY) ^{1}H NMR was carried out to determine change in diffusion on formation of higher assemblies. With increase in size, diffusion coefficient decreases due to slower rate of diffusion of bigger particles, indicating aggregate formation[29–31]. We observed decrease in diffusion coefficient from 6.61×10^{-10} m^2 s^{-1} to 6.15×10^{-10} m^2 s^{-1} as concentration increased from 6 mM to 150 mM (Fig. 4c). This confirms the change in size of molecular assemblies formed by L-Phe, as also shown by DLS. This small change in diffusion coefficient is

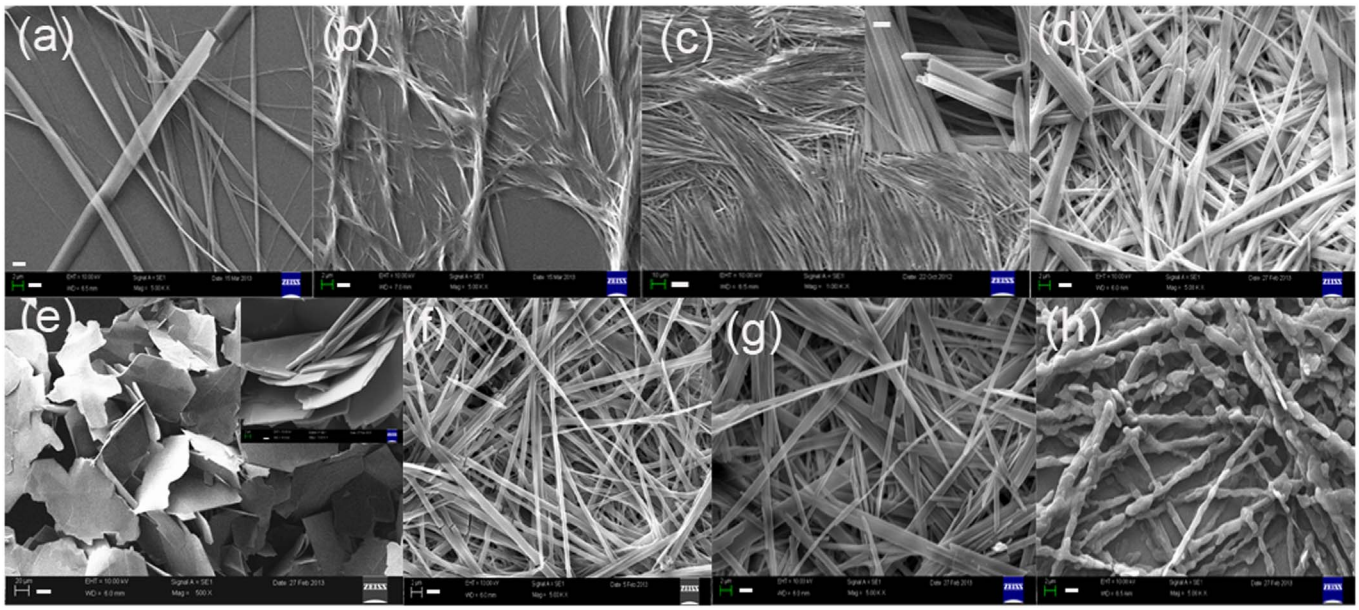

Figure 3 | Scanning electron micrographs of Phe (a) 300 μM L-Phe (b) 6 mM L-Phe (c) 300 mM L-Phe (top window 10 k × zoom) (d) D-Phe (e) DL-Phe (top window 5 k × zoom) (f) L-Phe in PBS (g) L-Phe in 0.1 N HCl (h) L-Phe in 0.1 N NaOH. Scale bars shown in white for (a), (b), (d), (f–h) are 2 μm; 10 μm for c and 20 μm for e.

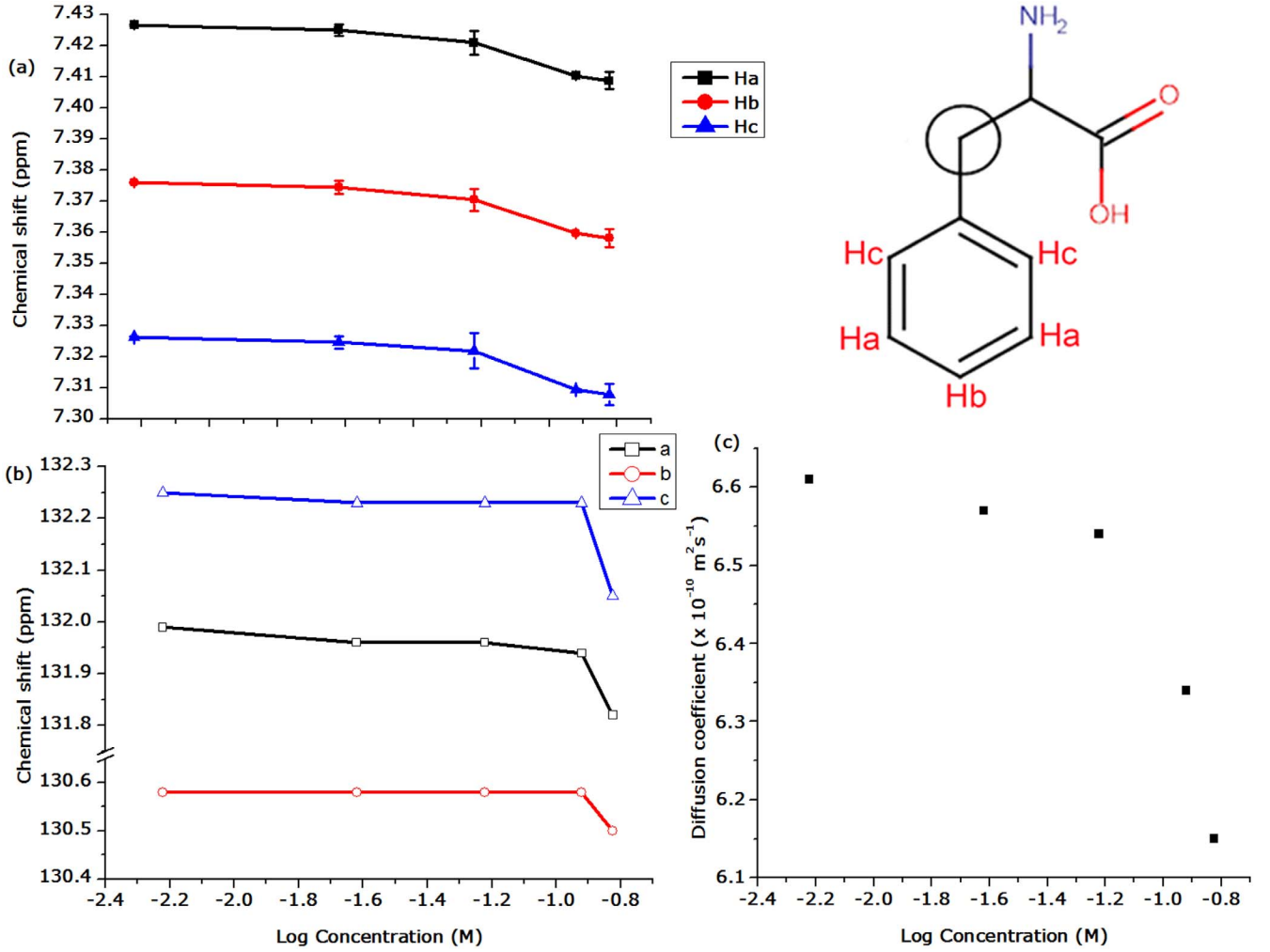

Figure 4 | Nuclear Magnetic Resonance (a) ^{1}H Chemical shift (δ, ppm) of aryl protons (Ha, Hb and Hc) with change in concentration from 1 mM to 150 mM (log scale) in ^{1}H NMR (b) ^{13}C chemical shift (ppm) of phenyl ring carbons (c) Change in diffusion coefficient with concentration in DOSY ^{1}H NMR.

considerable as similar change was observed for self-association of amyloid β (12–28) peptide[32].

In order to further highlight the involvement of hydrophobic interactions, effect of temperature and ionic strength was studied. With increasing temperature and ionic strength, increase in particle size was observed (Fig. 5). High temperature favoured formation of higher order assemblies at 60 mM concentration of L-Phe (Fig. 5a) due to increase in hydrophobic interactions[33,34]. With increase in ionic strength, particle size increased due to salt induced charge suppression, leading to effective hydrophobic interactions[35,36].

The uniqueness of L-Phe to form fibrous gel was further assessed by investigating the behaviour of alpha-phenylglycine (PG) and N-acetyl-L-phenylalanine methyl ester (Ac-Phe-OMe). PG is the smallest aromatic amino acid and differs from Phe by the absence of one methylene group attached to phenyl ring (Supplementary Fig. S6). Excitingly, this amino acid at saturated concentration (50 mM) did not yield fibrous gel. Also, rate of change of the chemical shift of methylene group protons (He and Hf) and Cα-H (Hd) proton with respect to change in concentration (Δδ/ΔC) clearly suggest the involvement of these protons in self-assembly (Supplementary Fig. S7). Lack of methylene group might be responsible for inability of PG to form gel. Ac-Phe-OMe is protected at N-terminus and C-terminus to avoid electrostatic interaction mediated self-assembly and only allow hydrophobic ring to involve in self-assembly process. Interestingly, this derivative gave rise to ThT positive assemblies at different concentrations as observed in Phe (Supplementary Fig. S8). Moreover other amino acids such as glutamine, tyrosine, tryptophan, DOPA (3,4-dihydroxyphenylalanine) and proline also failed to form gel at respective saturated concentrations under similar conditions (unpublished data). Considering all data, linear correlation was observed for change in ^{1}H chemical shift, light scattering, particle size and ThT binding with respect to concentration representing L-Phe self-assembly process (Fig. 6). Although techniques compared have different working principal, but relative variation of data with concentration is comparable, resulting in good correlation. As compared to L-Phe; PG and L-Gln did not show ThT fluorescence at different concentrations. As a result there is no change with increasing concentration. Inability of L-Phe to self-assemble in presence of GuHCl, also resulted in no change in ThT intensity with increasing concentration.

L-Phe aggregation modulation by D-Phe. Non-natural amino acids have shown potential as aggregation inhibitors by disrupting fibril formation of proteins like tau in Alzheimer's disease[37]. Also, D-amino acids have shown inhibitory effects on biofilm development having amyloid like characteristics[38,39]. So, based on the available evidence of inhibitory effects of D-enantiomers, we wanted to test the effect of D-Phe on L-Phe fibril formation. First we investigated behaviour of D-Phe alone. Notably, we observed gel formation in water (Fig. 3d) and in PBS (Supplementary Fig. S9a), as was observed

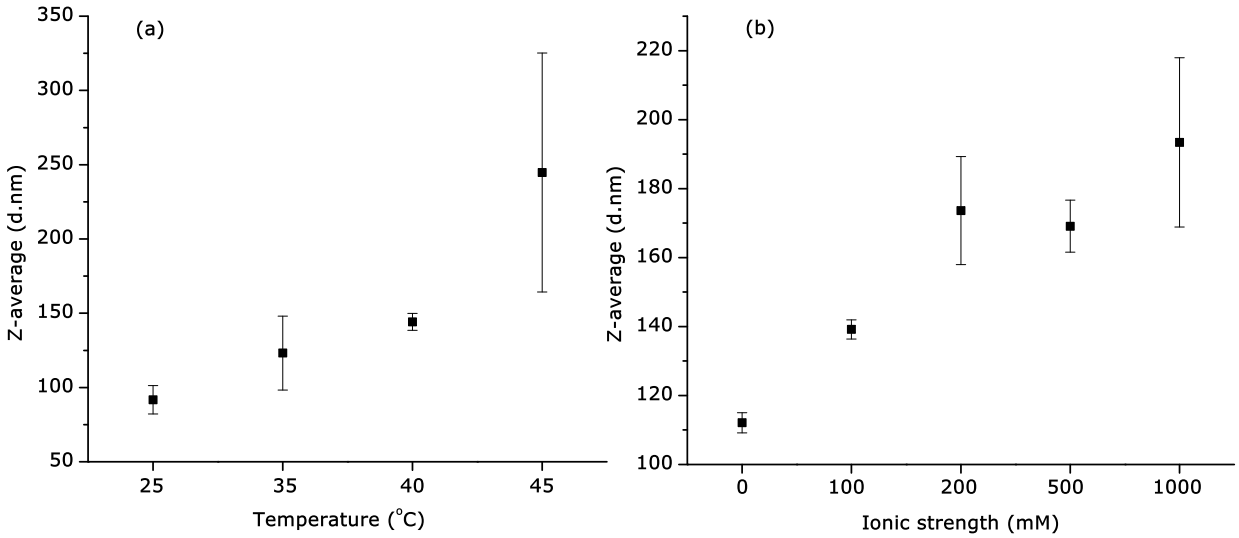

Figure 5 | Dynamic light scattering (a) Effect of temperature on L-Phe at 60 mM concentration (b) Effect of ionic strength on L-Phe at 72 mM concentration.

in L-Phe at 300 mM concentration with similar morphology (Fig. 3d). But when L-Phe was mixed with D enantiomer in equimolar ratio, this combination inhibited the formation of gel and some particles appeared which phased out from the solution (Fig. 2b). More importantly, morphology of aggregates formed by DL-Phe (racemate) was completely different from pure enantiomer, with flat surface and irregular edges appearing as flakes, unlike thread like fibrils (Fig. 3e and Supplementary Fig. S9b). These assemblies were arranged in layers with approximately 1–2 μm width and 100–200 μm length. DL-Phe showed similar ANS fluorescence as shown by L-Phe with blue shift at saturated concentration (Supplementary Fig. S4). This is probably due to the presence of more hydrophobic patches where ANS binds with high affinity[23]. We have also observed slightly higher negative Gibbs free energy (ΔG) of DL-Phe flakes formation as compared to L-Phe fibre formation, indicating more stability of flakes over fibres (Supplementary Fig. S10).

To further disclose the inhibitory effect of D-Phe on L-Phe self-assembly, we have titrated L-Phe with increasing amount of D-Phe. Interestingly, presence of ≥ 8% of D-Phe prevented fibre formation, and the flakes were formed as observed in the racemic mixture (Supplementary Table S1; Fig. S11a and S11b). Heterochiral seeding always resulted in flakes whereas homochiral seeding resulted in quick transition to fibrillar gel (methods section). After demonstrating the ability of D-Phe to perturb fibrillar assemblies of L-Phe, we investigated the capability of the flakes to propagate in L-Phe solution through seeding mechanism. We have observed no change in soluble Phe concentration when it was incubated with flakes as compared to L-Phe without flakes (Fig. 7 and Table S2). Remarkably, this reveals the incapability of the flakes to propagate further. SEM images also corroborates with this data where mixed morphology was observed at low seeding and flakes at higher seeding amounts (Supplementary Fig. S11c and S11d).

Discussion

We have demonstrated the ability of Phe to self-assemble into amyloid like fibrils relevant to PKU. Phe starts self-assembling at a very low concentration with positive ThT binding indicating their amyloidic nature. Light scattering, ThT fluorescence and particle size increased with increasing concentration. As compared to L-Gln, at 120 mM, seven fold ThT fluorescence and 40 fold light scattering enhancement was observed in L-Phe. It suggests that L-Phe has higher propensity to form higher order assemblies. Moreover, Phe transforms to gel at 300 mM concentration in both water and PBS.

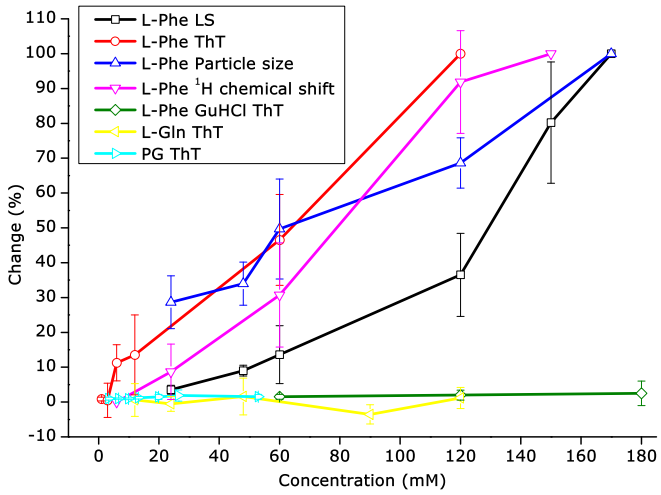

Figure 6 | Correlation of percent change reflecting self-assembly obtained from different techniques with change in concentration.

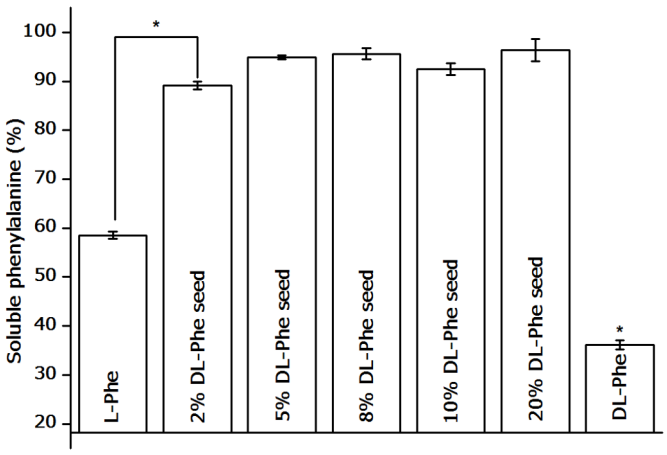

Figure 7 | Percentage of soluble Phe left after seeding with different amounts of DL-Phe flakes (significant $p < 0.05$). L-Phe and DL-Phe were not seeded.

Our finding confirms that L-Phe is capable to self-assemble at a wide range of concentrations and can transit to a gel state at high concentrations.

Upon investigating the structural features of L-Phe with SEM, we have observed fibrous assemblies formed at wide range of pH. At extreme pH, gel formed slowly as compared to that in water and PBS, which might be due to charge-charge repulsion. But finally gel formation under these conditions suggests that electrostatic interactions are not the major drivers, but hydrophobic interactions between Phe rings might be playing major role in self-assembling process.

This is further supported by the use of neutral end capped Phe derivative, Ac-Phe-OMe as a stringent control. Self-association of this molecule into ThT positive assembly revealed the importance of hydrophobic interactions. Moreover, increase in particle size with increase in ionic strength and temperature strengthens the involvement of hydrophobic interactions[33–36]. Interestingly, the inability of PG to form gel clearly indicates that methylene group in Phe provides more flexibility, hydrophobicity and orientation to ring structure to favour stacking interactions to form fibrous gel. Concentration dependent ^{1}H and ^{13}C NMR analysis of Phe, further confirms the role of Phe ring in self-assembly process. Upfield chemical shift was observed which is attributed to the stacking intermolecular interactions between π-electron cloud of Phe ring, resulting in shielding and this effect becomes prominent at high concentration[28,40]. Additionally, increase in particle size and decrease in diffusion coefficient was observed in ^{1}H DOSY experiment indicating the formation of higher order assemblies. The values obtained from ^{1}H, ^{13}C and DOSY experiments corroborates well to L-Phe self-assembly with increase in concentration. Remarkably, with increasing concentration of Phe, linear correlation was observed for change in light scattering, particle size, chemical shift and ThT fluorescence. This not only authenticates the data obtained using different techniques but further validates the major role of hydrophobic interactions in driving self-assembly. Moreover, L-Phe in presence of GuHCl, L-Gln and PG failed to show similar correlation, which further confirms the unique nature of self-assembly of L-Phe. These results corroborates well with toxicity data obtained from cell lines incubated with increasing concentration of L-Phe[5]. No comparable change in ThT fluorescence by PG and no absorbance at 450 nm and emission at 489 nm by Phe rules out the possibility of any interference to ThT fluorescence, as shown by few other small molecules[41]. Further, ThT binding to Phe fibrils was earlier shown by confocal microscopy[5].

It is known that chirality plays crucial role in deciding fate of peptide self-assembly as observed in a tripeptide LFF, which do not form fibres/gel. But substitution of L-Leu with D-Leu resulted in self-assembly of this peptide to hydrogel with fibrous morphology[42]. Similar effect of chirality induction is reported in glutamic acid amphiphiles, forming different helical tubes in pure enantiomer state and nanosheets as racemic mixture[43]. Interestingly D-Phe forms gel with fibrous morphology similar to L-Phe. Moreover, in presence of equimolar D-Phe, racemate formed flakes rather than fibrous gel. This seems to be interesting as we were able to tweak the aggregation pathway of L-Phe by using its enantiomer counterpart. Presence of both enantiomers counteracts each other's ability to form gel. If the cell toxicity observed in PKU is owing to fibrous assemblies[5], then having a strategy of inhibiting fibre formation might be a good approach, as applied in other amyloid diseases. Interestingly, as compared to self-assembly kinetics of pure enantiomers shown by ThT binding, DL-Phe showed slightly higher fluorescence. This might be due to different extent of packing interactions between flakes and fibres as shown previously by Zhu *et al.*, that D and L enantiomer of glutamic acid based lipids in racemic mixture form strong hydrogen bonds[43]. More negative free energy for DL-Phe flakes partly explains the favourable transition to flakes rather than to fibrous gel. Also, the flakes formed are non-propagating and does not seed L-Phe, thus preventing it's self-assembly. Further investigation is required to know complete structural differences between fibrous gel and flakes at atomic level.

So based on our observations, we hypothesize the use of D-Phe amino acid as a potential therapeutic molecule in PKU. Due to defective phenylalanine hydroxylase, level of L-Phe in the brain increases, leading to L-Phe self-assembly by hydrophobic interactions to form toxic amyloid fibrils. If D-Phe is administered, it may act in two ways on L-Phe. 1) Monomers of D-Phe will interact with L-Phe monomers and convert the fibrous formation path of L-Phe to flakes. This may happen quicker than the fibre formation from individual enantiomer as supported by our kinetic and stability data of fibre and flake formation. 2) The flakes formed will now further restrict fibre formation tendency of L-Phe due to their non-propagating nature. These steps will save neurons from toxicity caused by Phe fibres[5]. Similar approaches of slowing down the aggregation or constraining the toxic fibril formation to different pathways are employed in other amyloid diseases[44]. Additionally, D-Phe might compete for the transporters used by L-Phe[45] to cross blood brain barrier (BBB) and limits its entry as observed in case of LNAA therapy[2,46] (Fig. 8). Now, these findings need validation in cell lines and animal models of phenylketonuria.

In summary, the self-assembly process of Phe was characterized by NMR, light scattering, particle size analysis, SEM imaging, ThT and ANS binding. Phe has shown peculiarity to form fibrous gel, while other amino acids tested failed to do so. We have shown that fibrous gel formation tendency by Phe is not only due to already described hydrogen bonding and ionic interactions, but hydrophobic interactions play a major role in driving the self-assembly process. We have also revealed the capability of D-Phe to tweak L-Phe fibrous state to flakes which are incapable to propagate further and unable to seed L-Phe. Therefore, we propose the use of D-Phe as therapeutic molecule in PKU. D-Phe and DL-Phe can now be tested in cell culture and animal model of PKU for their own toxicity and to confirm their ability to prevent toxicity caused by L-Phe fibres. Overall, this work provides additional therapeutic approach to currently available low Phe diet and LNAA therapy. The kinetic and mechanistic details at molecular level revealed in this study can be used for screening and rationally designing compounds to target aggregation in PKU[47–49]. Phe fibres and flakes can also be used as a model system to elucidate the pathological effects relevant to other amyloid diseases.

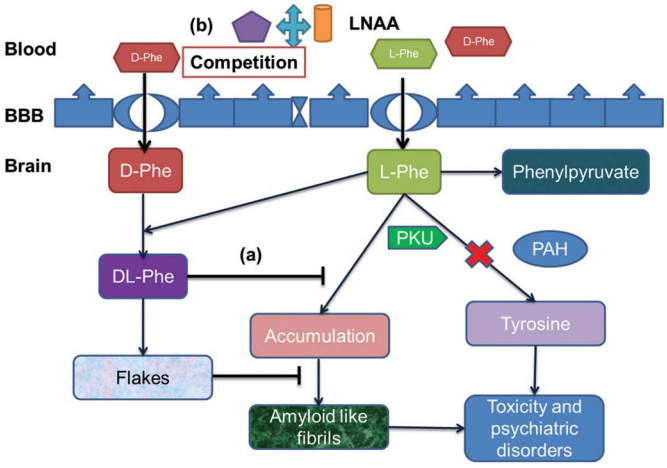

Figure 8 | Proposed mechanism of D-Phe action on L-Phe in phenylketonuria (a) Inhibition of amyloid formation by D-Phe (b) Competition of D-Phe for L-Phe transporter as described for large neutral amino acids (LNAA).

Methods

Materials. L-Phe and D-Phe were purchased from Sisco Research Laboratories, L-Gln from HIMEDIA, Ac-Phe-OMe from Bachem and L-(+)-α-phenylglycine (PG) from Sigma. HPLC grade water and acetonitrile (ACN) were purchased from Merck and Trifluoroacetic acid (TFA) from Thermo Scientific. ThT and 8-anilino-1-naphthalenesulfonic acid (ANS) were purchased from Sigma and phosphate buffered saline (PBS) from Fisher Scientific. All experiments in this study were repeated twice and mean ± standard deviation (s.d.) values obtained were reported.

Self-assembly of phe. Different concentrations of Phe ranging from 300 μM to 170 mM were prepared by dissolving appropriate amount in double distilled water (water) at room temperature. The saturated solution of L-Phe and D-Phe were prepared by dissolving 50 mg in 1 mL water (300 mM) at 70 °C for 18–24 h. Similarly the saturated solution of DL-Phe (50 : 50 racemate) was prepared by dissolving L-Phe (25 mg) and D-Phe (25 mg) in 1 mL water at 70 °C for 18–24 h. The solution was then transferred to a fresh vial and allowed to cool at room temperature without disturbing. Additionally, saturated solution of L-Phe (300 mM) was mixed with saturated solution of D-Phe (300 mM) in 1 : 1 (v/v) ratio. The pH dependence aggregation of Phe was studied in water (pH 5.5); PBS (pH 7.4); 0.1 N HCl (pH 1.3) and 0.1 M NaOH (pH 13).

RP-HPLC analysis. An aliquot of an ongoing aggregation reaction was subjected to centrifugation at 305,611×g for 2 h. 30 μL supernatant was subjected for analysis at 215 nm wavelength on Agilent HPLC 1260 using ZORBAX Eclipse Plus C18 Rapid Resolution (4.6 × 100 mm, 3.5 μm) column with water (mobile phase A) and acetonitrile (mobile phase B) containing 0.05% TFA at flow rate of 1 mL min^{-1} for 20 minutes. Mobile phase B was increased from 0–30% in 10 minutes and Phe eluted at 6.0 ± 0.3 minute between 8.8–10.25% of mobile phase B.

90° LS, DLS and ThT binding fluorescence assay. LS and ThT experiments were performed on Perkin Elmer LS55 Fluorescence Spectrometer. For LS, excitation and emission wavelength was kept at 450 nm with slit width of 2.5 nm and 5 nm respectively and voltage at 650 V. For ThT assay, excitation wavelength was 450 nm with slit width of 5 nm and emission wavelength was 489 nm with slit width of 10 nm at 650 V[19]. Final concentration of ThT in the sample was kept at 200 μM. Average of three readings compiled from two independent experiments was reported here and subtracted from blank. For highly concentrated samples, experiments were carried out in continuous monitoring mode. 10–15 minutes were sufficient to get signal saturated due to the presence of high amount of fibres. For same samples, DLS was carried out at 25 °C on Malvern Zetasizer Nano ZS90 with 632.8 nm laser at 90° scattering angle. Sample was filtered through 0.2 μm filter and kept at room temperature for 2 hours before analysis. Samples were analysed at different temperatures and ionic strength.

Scanning electron microscopy (SEM). 10 μL of aggregated sample was transferred to a glass cover slip, air dried and coated with gold/palladium alloy with the help of SC7620 sputter coater. The sample was imaged using Carl Zeiss EVO18 electron microscope kept at 10 kV. Multiple images of the same sample were taken and representative image is reported here.

Nuclear magnetic resonance (NMR). All spectra were collected on a Bruker 800-MHz NMR spectrometer equipped with a triple-resonance TCI (^{1}H, ^{13}C,^{15}N, and^{2}H lock) cryogenic probe. All 1D ^{1}H NMR (noesypr1d in Bruker library) spectra with water suppression were recorded with 64 scans, 64 K data points, spectral width of 20 ppm, relaxation delay 5 second. All 1D spectra were processed with line broadening of 0.3 Hz, manually phase and baseline corrected. The chemical shifts were internally calibrated to the Trimethylsilyl propionate (TSP) peak at 0.0 ppm. ^{1}H-^{13}C phase sensitive (echo/antiecho) heteronuclear single quantum correlation (HSQC) experiments were recorded with inverse detection and ^{13}C decoupling. A relaxation delay of 2 seconds was used. A total of 2048 data points were acquired and a total of 8 scans were averaged for each of 256 increments, with spectral widths of 16 and 180 ppm in ^{1}H and ^{13}C dimensions respectively. For the ^{1}H-^{13}C HSQC zero filling up to 1 k data points and forward linear prediction up to 128 points were used in t_1 dimensions and multiplication by shifted sine-bell squared apodization function were used in both t_2 and t_1 dimension prior to Fourier transform. For 2D DOSY ^{1}H NMR, stimulated echo bipolar gradient pulse experiments were used with a pulse delay of 5 ms after each gradient, a pulse field gradient length of 2.2 ms and with 15 s relaxation decay[50]. Chemical shift (δ, ppm) and diffusion coefficient (m^2 s^{-1}) was plotted against log concentration (molar).

L-Phe titration with D-Phe. To understand the effect of one enantiomer on another, we titrated saturated solution of L-Phe with 0%, 5%, 20% and 50% D-Phe solution to monitor the minimum amount required to see the impact on aggregation. Similarly effect of DL-Phe on L-Phe aggregation was studied.

Homochiral and Heterochiral seeding. For seeding experiment, the final aggregated solution of L-Phe, D-Phe and DL-Phe was taken and 10% (w/w) was transferred to a fresh saturated solution of own or another enantiomer. The concentration of solution before addition and after completion of the aggregation was checked by RP-HPLC. In this experiment, homochiral seeding is seeding of L-Phe solution with L-Phe seed and heterochiral seeding is seeding of L-Phe solution with D-Phe or DL-Phe seed. Statistical significance was predicted by applying two-tailed student's t-test [*, $P < 0.05$ is considered significant].

1. Blau, N., van Spronsen, F. J. & Levy, H. L. Phenylketonuria. *Lancet* **376**, 1417–1427 (2010).
2. Williams, R. A., Mamotte, C. D. & Burnett, J. R. Phenylalanine: an inborn error of phenylalanine metabolism. *Clin. Biochem. Rev.* **29**, 31–41 (2008).
3. Mitchell, J. J., Trakadis, Y. J. & Scriver, C. R. Phenylalanine hydroxylase deficiency. *Genet. Med.* **13**, 697–707 (2011).
4. Kaufman, S. A model of human phenylalanine metabolism in normal subjects and in phenylketonuric patients. *Proc. Natl. Acad. Sci. U. S. A.* **96**, 3160–3164 (1999).
5. Adler-Abramovich, L. *et al.* Phenylalanine assembly into toxic fibrils suggests amyloid etiology in phenylketonuria. *Nat. Chem. Biol.* **8**, 701–706 (2012).
6. Eisenberg, D. & Jucker, M. The amyloid state of proteins in human diseases. *Cell* **148**, 1188–1203 (2012).
7. Stefani, M. Protein misfolding and aggregation: new examples in medicine and biology of the dark side of the protein world. *Biochim. Biophys. Acta* **1739**, 5–25 (2004).
8. Greenwald, J. & Riek, R. Biology of amyloid: structure, function and regulation. *Structure* **18**, 1244–1260 (2010).
9. Hsu, W.-P., Koo, K.-K. & Myerson, A. S. The gel-crystallization of 1-phenylalanine and aspartame from aqueous solutions. *Chem. Eng. Commun.* **189**, 1079–1090 (2002).
10. Olsztynska, S., Dupuy, N., Vrielynck, L. & Komorowska, M. Water evaporation analysis of L-phenylalanine from initial aqueous solutions to powder state by vibrational spectroscopy. *Appl. Spectrosc.* **60**, 1040–1053 (2006).
11. Olsztynska, S. & Komorowska, M. Conformational Changes of L-phenylalanine induced by near infrared radiation. ATR-FTIR studies. *Struct. Chem.* **23**, 1399–1407 (2012).
12. Guo, C., Luo, Y., Zhou, R. & Wei, G. Probing the self-assembly mechanism of diphenylalanine-based peptide nanovesicles and nanotubes. *ACS Nano* **6**, 3907–3918 (2012).
13. Gazit, E. A possible role for pi-stacking in the self-assembly of amyloid fibrils. *FASEB J.* **16**, 77–83 (2002).
14. Levy, M., Garmy, N., Gazit, E. & Fantini, J. The minimal amyloid-forming fragment of the islet amyloid polypeptide is a glycolipid-binding domain. *FEBS J.* **273**, 5724–5735 (2006).
15. Huang, R. *et al.* NMR characterization of monomeric and oligomeric conformations of human calcitonin and its interaction with EGCG. *J. Mol. Biol.* **416**, 108–120 (2012).
16. Tu, L. H. & Raleigh, D. P. Role of aromatic interactions in amyloid formation by islet amyloid polypeptide. *Biochemistry* **52**, 333–342 (2013).
17. Boyd-kimball, D., Abdul, H. M., Reed, T., Sultana, R. & Butterfield, D. A. Role of phenylalanine 20 in alzheimer's amyloid β-peptide (1–42)-induced oxidative stress and neurotoxicity. *Chem. Res. Toxicol.* **17**, 1743–1749 (2004).
18. Kar, K., Jayaraman, M., Sahoo, B., Kodali, R. & Wetzel, R. Critical nucleus size for disease-related polyglutamine aggregation is repeat-length dependent. *Nat. Struct. Mol. Biol.* **18**, 328–336 (2011).
19. Chen, S., Berthelier, V., Hamilton, J. B., O'Nuallain, B. & Wetzel, R. Amyloid-like features of polyglutamine aggregates and their assembly kinetics. *Biochemistry* **41**, 7391–7399 (2002).
20. Zhang, S., Marini, D. M., Hwang, W. & Santoso, S. Design of nanostructured biological materials through self-assembly of peptides and proteins. *Curr. Opin. Chem. Biol.* **6**, 865–871 (2002).
21. Griffith, E. C. & Vaida, V. Ionization state of L-phenylalanine at the air-water interface. *J. Am. Chem. Soc.* **135**, 710–716 (2013).
22. Gasymov, O. K. & Glasgow, B. J. ANS fluorescence: potential to augment the identification of the external binding sites of proteins. *Biochim. Biophys. Acta* **1774**, 403–411 (2007).
23. Gabellieri, E. & Strambini, G. B. ANS fluorescence detects widespread perturbations of protein tertiary structure in ice. *Biophys. J.* **90**, 3239–3245 (2006).
24. Lindgren, M., Sorgjerd, K. & Hammarstrom, P. Detection and characterization of aggregates, prefibrillar amyloidogenic oligomers, and protofibrils using fluorescence spectroscopy. *Biophys. J.* **88**, 4200–4212 (2005).
25. Yousefi, R. *et al.* Investigation on the surface hydrophobicity and aggregation kinetics of human calprotectin in the presence of calcium. *J. Biochem. Mol. Biol.* **38**, 407–413 (2005).
26. Castellino, F. J. & Barker, R. The Effect of guanidinium, carbamoylguanidinium, and guanylguanidinium salts on the solubility of benzoyl-L-tyrosine ethyl ester and acetyltetraglycine ethyl ester in water. *Biochemistry* **8**, 3439–3442 (1969).
27. England, J. L. & Haran, G. Role of solvation effects in protein denaturation: from thermodynamics to single molecules and back. *Annu. Rev. Phys. Chem.* **62**, 257–277 (2011).
28. Bonechi, C., Martini, S., Magnani, A. & Rossi, C. Stacking interaction study of trans-resveratrol (trans-3,5,4′-trihydroxystilbene) in solution by nuclear magnetic resonance and fourier transform infrared spectroscopy. *Magn. Reson. Chem.* **46**, 625–629 (2008).
29. Soong, R., Brender, J. R., MacDonald, P. M. & Ramamoorthy, A. Association of highly compact type II diabetes related islet amyloid polypeptide intermediate

species at physiological temperature revealed by diffusion NMR spectroscopy. *J. Am. Chem. Soc.* **131**, 7079–7085 (2008).
30. Cohen, Y., Avram, L. & Frish, L. Diffusion NMR spectroscopy in supramolecular and combinatorial chemistry: an old parameter-new insights. *Angew. Chem. Int. Ed.* **44**, 520–554 (2005).
31. Macchioni, A., Ciancaleoni, G., Zuccaccia, C. & Zuccaccia, D. Determining accurate molecular sizes in solution through NMR diffusion spectroscopy. *Chem. Soc. Rev.* **37**, 479–489 (2008).
32. Mansfield, S. L., Jayawickrama, D. A., Timmons, J. S. & Larive, C. K. Measurement of peptide aggregation with pulsed-field gradient nuclear magnetic resonance spectroscopy. *Biochim. Biophys. Acta* **1382**, 257–265 (1998).
33. Schellman, J. A. Temperature, stability, and the hydrophobic interaction. *Biophys. J.* **73**, 2960–2964 (1997).
34. Chandler, D. Interfaces and the driving force of hydrophobic assembly. *Nature* **437**, 640–647 (2005).
35. Castelletto, V., Hamley, I. W., Cenker, C. & Olsson, U. Influence of salt on the self-assembly of two model amyloid heptapeptides. *J. Phys. Chem. B* **114**, 8002–8008 (2010).
36. Hu, Y. *et al.* Dye Adsorption by resins: Effect of ionic strength on hydrophobic and electrostatic interactions. *Chem. Eng. J.* **228**, 392–397 (2013).
37. Sievers, S. A. *et al.* Structure-based design of non-natural amino-acid inhibitors of amyloid fibril formation. *Nature* **475**, 96–100 (2011).
38. Hochbaum, A. I. *et al.* Inhibitory effects of D-amino acids on *Staphylococcus aureus* biofilm development. *J. Bacteriol.* **193**, 5616–5622 (2011).
39. Cegelski, L. *et al.* Small-molecule inhibitors target *Escherichia coli* amyloid biogenesis and biofilm formation. *Nat. Chem. Biol.* **5**, 913–919 (2009).
40. Sanna, C. *et al.* New class of aggregates in aqueous solution: An NMR, thermodynamic, and dynamic light scattering study. *Langmuir* **22**, 6031–6041 (2006).
41. Suzuki, Y., Brender, J. R., Hartman, K., Ramamoorthy, A. & Marsh, E. N. Alternative pathways of human islet amyloid polypeptide aggregation distinguished by (19)f nuclear magnetic resonance-detected kinetics of monomer consumption. *Biochemistry* **51**, 8154–8162 (2012).
42. Marchesan, S. *et al.* Unzipping the role of chirality in nanoscale self-assembly of tripeptide hydrogels. *Nanoscale* **4**, 6752–6760 (2012).
43. Zhu, X., Li, Y., Duan, P. & Liu, M. Self-assembled ultralong chiral nanotubes and tuning of their chirality through the mixing of enantiomeric components. *Chemistry* **16**, 8034–8040 (2010).
44. Cheng, B., Gong, H., Xiao, H., Petersen, R. B., Zheng, L. & Huang, K. Inhibiting toxic aggregation of amyloidogenic proteins: A therapeutic strategy for protein misfolding diseases. *Biochim. Biophys. Acta* **1830**, 4860–4871 (2013).
45. Yanagida, O. *et al.* Human L-type amino acid transporter 1 (LAT1): characterization of function and expression in tumor cell lines. *Biochim. Biophys. Acta* **1514**, 291–302 (2001).
46. Van Spronsen, F. J., de Groot, M. J., Hoeksma, M., Reijngoud, D. & van Rijn, M. Large neutral amino acids in the treatment of PKU: from theory to practice. *J. Inherit. Metab. Dis.* **33**, 671–676 (2010).
47. Ramamoorthy, A. & Lim, M. H. Structural characterization and inhibition of toxic amyloid-beta oligomeric intermediates. *Biophys. J.* **105**, 287–288 (2013).
48. Braymer, J. *et al.* Development of bifunctional stillbene derivatives for targeting and modulating metal-amyloid-beta species. *Inorg. Chem.* **50**, 10724–10734 (2011).
49. Detoma, A. S., Salamekh, S., Ramamoorthy, A. & Lim, M. H. Misfolded proteins in alzheimer's disease and type II diabetes. *Chem. Soc. Rev.* **41**, 608–621 (2012).
50. Wu, D. H., Chen, A. D. & Johnson, C. S. An improved diffusion-ordered spectroscopy experiment incorporating bipolar-gradient pulses. *J. Magn. Reson. Series A* **115**, 260–264 (1995).

Acknowledgments

This work is done with the financial support given to A.K.T. by Department of Biotechnology, Government of India Grant (BT/PR3041/NNT/28/545/2011) and IIT Kanpur research initiating grant (IITK/BSBE/20100226). V.S. and R.K.R gratefully acknowledges financial support from the Council of Scientific and Industrial Research, India. We thank Prof. DS Katti for providing SEM facility procured under CARE grant of IITK. A.K.T. thanks his former M.Tech student Itika Saha for timely highlighting the role of Phe amyloid formation in PKU to V.S. A.K.T. gratefully acknowledges Prof. Pradip Sinha and Mainak Das for consistent encouragement.

Author contributions

The experiments were designed by V.S. and A.K.T. The experimental work was performed by V.S. NMR experiments were done by R.K.R, N.S. and A.A. The manuscript was written by V.S. and A.K.T. A.K.T. conceived & directed the ideas, planning and overall execution.

Additional information

Supplementary information accompanies this paper at http://www.nature.com/scientificreports

Competing financial interests: The authors declare no competing financial interests.

How to cite this article: Singh, V., Rai, R.K., Arora, A., Sinha, N. & Thakur, A.K. Therapeutic implication of L-phenylalanine aggregation mechanism and its modulation by D-phenylalanine in phenylketonuria. *Sci. Rep.* **4**, 3875; DOI:10.1038/srep03875 (2014).

This work is licensed under a Creative Commons Attribution-NonCommercial-NoDerivs 3.0 Unported license. To view a copy of this license, visit http://creativecommons.org/licenses/by-nc-nd/3.0